Advanced Diagnostic Facility for Low-Density Plasma Characterization

IEPC-2024-288

Presented at the 38th International Electric Propulsion Conference
Pierre Baudis Convention Center • Toulouse, France
June 23-28, 2024

Pavel Smirnov[1], Ruslan Kozakov[2] and Jochen Schein[3]
Universität der Bundeswehr München, Institute of Physics and Plasma Technology, Neubiberg, 85521, Germany

Luca Henrich[4], Erik Jozsef[5] and Chris Volkmar[6]
University of Applied Sciences, Center of Competence for Nanotechnology and Photonics, Giessen, 35390, Germany

Abstract: The paper describes activities of the institute of Physics and plasma technology to establish a reliable plasma diagnostic facility for the characterization of electric thrusters. The probe diagnostic setup, which includes Langmuir probes, emissive probes, and a retarding potential analyser, has been enhanced with a non-intrusive optical diagnostic setup incorporating Rayleigh and Thomson scattering techniques. The sensitivity limit of the optical diagnostics was analysed and improved. Preliminary results from measurements on the low ionization degree plasma of a capacitively coupled radiofrequency thruster are presented.

Nomenclature

EP	=	electric propulsion
UniBwM	=	university of Bundeswehr Munich
REL	=	Radiofrequenz-antrieb-Entwicklungs Labor (Ger. - Laboratory of RF thruster development)
VP	=	Forevacuum pump
SMP	=	Roots pump
TMP	=	Turbomolecular pump
DC	=	direct current
AC	=	alternating current
OML	=	orbital motion limited
RPA	=	retarding potential analyser
ICCD	=	intensified charge coupled device
CW	=	continuous wave
RF	=	Radio Frequency

I.Introduction

THE determination of the plasma properties is the cornerstone of electric propulsion (EP) research and development, with probe diagnostic being probably the most reliable method to characterize plasma. With the set of the Langmuir and emissive probes, one can determine such plasma parameters as electron temperature, density and

[1] PhD student, Institute of Physics and Plasma Technology, pavel.smirnov@unibw.de
[2] Post-doc Researcher, Institute of Physics and Plasma Technology, ruslan.kozakov@unibw.de
[3] Professor, Institute of Physics and Plasma Technology, jochen.schein@unibw.de
[4] PhD student, Department of electrical engineering, luca.henrich@ei.thm.de
[5] PhD student, Department of electrical engineering, erik.jozsef@ei.thm.de
[6] Professor, Department of electrical engineering, chris.volkmar@ei.thm.de

plasma potential. Although this technique has proven itself in many studies, the interaction between the probes and the plasma introduces some uncertainty in these measurements.

Alternative methods for measuring plasma parameters have been proposed to address these uncertainties, notably optical diagnostics. Techniques such as Thompson and Rayleigh scattering could decrease the interference with the plasma while still providing reliable data. These methods have been demonstrated effectively in recent studies on hall effect thrusters[1,2].

Many novel EP systems utilise low-power discharge plasmas with low ionisation degrees. These plasmas are often accelerated with a magnetic nozzle, double layer, or a combination of both, utilizing volume outside its construction as an acceleration zone. Investigating such areas with a conventional probe diagnostic is not always possible, as the probes can cause critical disturbances in the plasma, compromising the results. Although such thrusters could benefit from the laser based optical diagnostic, it is a challenging task due to low electron densities and low pressures, which often fall outside the sensitivity ranges of these techniques.

The development of the plasma diagnostic facility is described in the presented paper. The diagnostic setup includes Langmuir probes, emissive probes, a retarding potential analyser, and a laser system for Rayleigh and Thomson scattering. This setup was installed and tested at the Southampton vacuum facility of the university of Bundeswehr Munich (UniBw M). The paper addresses sensitivity issues and discusses mitigation strategies, presenting preliminary measurement results on the capacitively coupled radiofrequency thruster C-Star plasma.

II. Experimental setup

This chapter provides short description of the experimental setup, namely the vacuum chamber and the thruster, as the object of measurement.

A. Southampton vacuum facility

"Southampton" is a vacuum facility for electric propulsion research under space related environmental conditions. It is located at REL (Radiofrequenz-antrieb-Entwicklungs Labor). The vacuum chamber has a volume of 1 m^3, it is 850 mm in diameter and ca. 2000 mm in length. The schematic and general view of Southampton facility are shown on fig. 1.

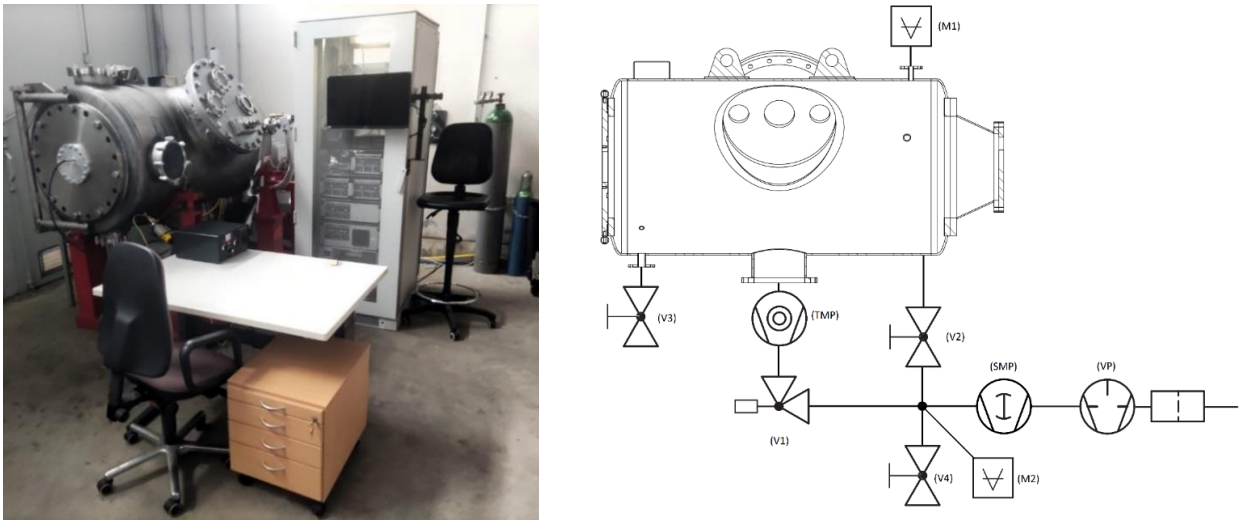

a) *b)*

Figure 1. Southampton vacuum facility. General view (a) and the schematic (b).

The pumping system consists of three levels:

- The first level is the fore-vacuum pump (VP) Pfeiffer DUO 125 with a pumping speed of 135 m^3/h. It is used for the initial pump-down phase from atmospheric pressure to 1E-2 mbar.
- The second level is the Roots pump (SMP) Pfeiffer Okta 250, which operates in the medium vacuum (under 10 mbar) and allows the facility to reach pressures below 1E-3 mbar with a pumping speed of up to 440 m^3/h. This level primarily speeds up the initial pumping phase and maintains low back pressure for the third pumping level during high propellant mass flows.
- The third level consists of a turbomolecular pump (TMP) Pfeiffer TPH 2200. The ultimate pressure of this stage is down to 8E-7 mbar with a pumping speed of up to 2200 l/s on nitrogen.

The facility is equipped with a two-line gas supply system, maintaining both thermal and pressure stability to ensure accurate propellant supply. Furthermore, the entire facility is fully automated, meaning all parameters, including vacuum levels, the status of pumps and valves, and propellant and electrical supply system parameters, are recorded and can be controlled remotely.

B. C-Star Thruster

The C-STAR is a capacitively coupled radiofrequency thruster developed at the University of Bundeswehr[3]. A radial alternating electrical field of several MHz in the discharge channel is primarily used for plasma generation in two circular discharge channels. Such plasma is normally positively charged with respect to electrodes. Due to the geometry of the thruster electrodes, the effect of a capacitive discharge asymmetry occurs, adding a DC component to the mainly AC discharge (creating a constant potential offset for the smaller electrode).

Permanent magnets in the thruster create an axial magnetic field in the discharge channel, which, interacting with the radial DC electric field, induces a tangential ExB drift. This drift occurs in opposite directions in each discharge channel, contributing to ionization.

The C-STAR generates thrust through a combination of electrothermal, electromagnetic, and electrostatic acceleration mechanisms. Electrons, as the lighter species, expand thermally to outer space, following the magnetic lines in axial direction. These electrons create a negatively charged layer, known as the electron double layer, acting as a virtual electrode and accelerating heavier ions behind them[4].

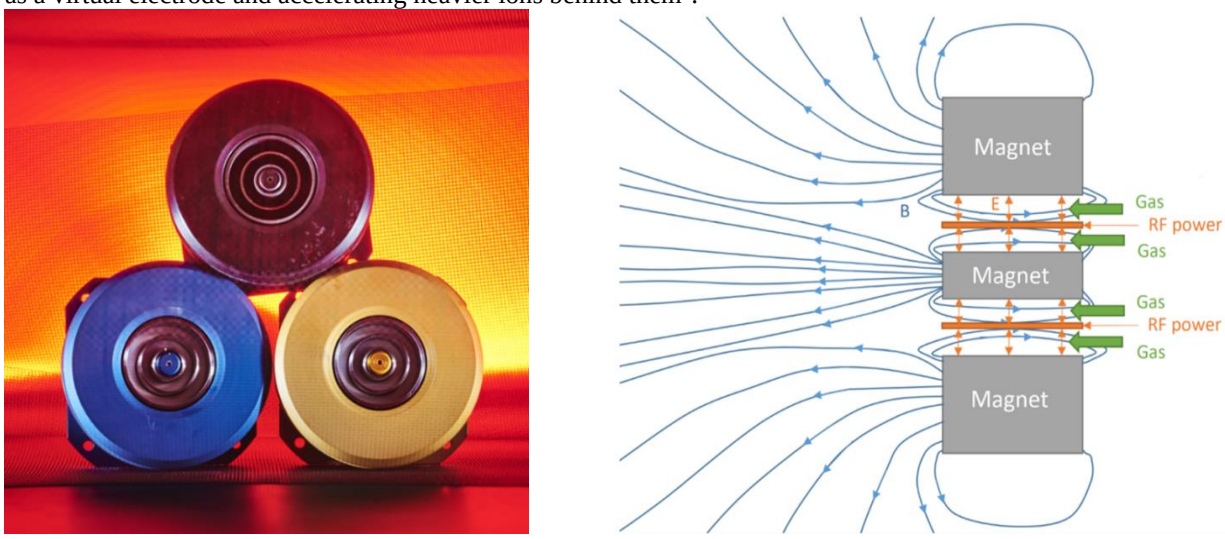

a) *b)*

Figure 2. C-STAR thruster. General view (a) and the schematic (b).

C. Experimental setup

To conduct a comprehensive analysis of the thruster's operation and its properties, it is essential to perform diagnostics with spatial resolution. Typically, moving the thruster during testing is undesirable due to uncertainties related to interactions between the thruster and the vacuum chamber. While installation of the probes on the moving arm is the common approach, optical diagnostic techniques require extensive deployment and calibration efforts, and the automated repositioning can cause vibrational misalignment.

To address this, the setup was designed to keep the diagnostic equipment static and mount the thruster on the moving platform. This configuration allows for a one-dimensional (1D) scan of plasma properties in the exhaust jet. The Langmuir and emissive probes, along with the optical diagnostics, are mounted on a stationary rectangular frame. The retarding potential analyser is positioned 500 mm further away to ensure it is outside the acceleration zone, allowing it to accurately characterize fully accelerated ions.

The experimental setup is depicted below:

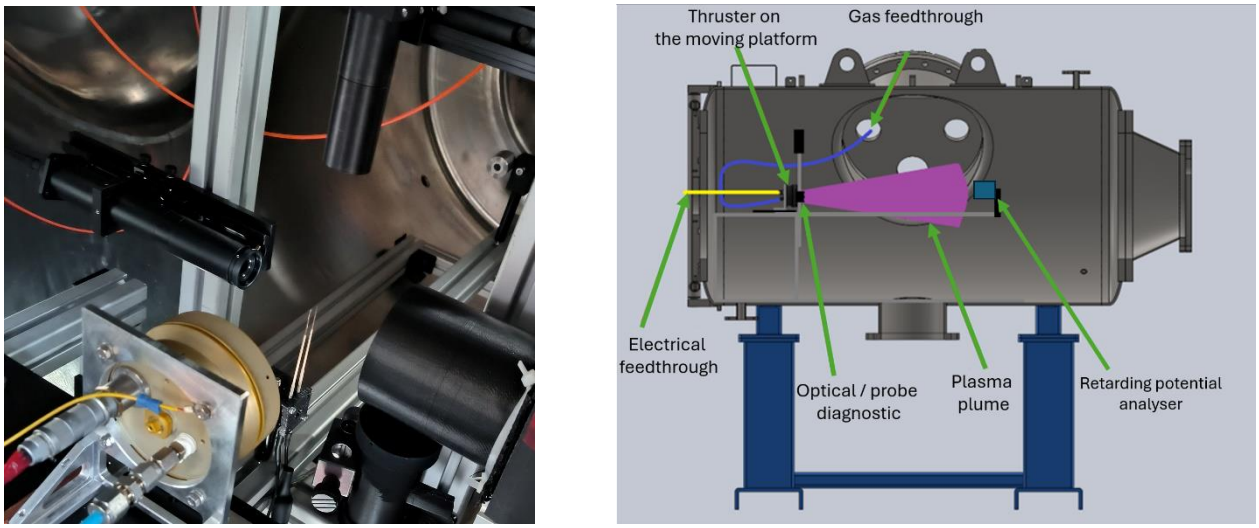

a) *b)*

Figure 3. Experimental setup. General view (a) and the schematic (b).

III. Probe diagnostic setup and preliminary results

This chapter describes the assembled plasma probe diagnostic, including Langmuir and emissive probes and the retarding potential analyser. The preliminary results of the measurements are provided, demonstrating the applicability of the probes for the radiofrequency discharge characterization.

A. Electric probes

A set of electric probes, consisting of an emissive probe and a Langmuir probe, was prepared (see Fig. 3). Due to the expected low electron densities in capacitively coupled RF discharge plasma, the Debye radius in the plume plasma is anticipated to be larger than the probe radius. Both probes are installed in a single fixture with a separation of 1 cm, positioned one after another. This arrangement allows for the measurements from both probes to be overlapped after several measurements in the axial direction. The probes are removed from the plasma plume when optical diagnostics are performed.

The objective of the Langmuir probe diagnostics is to determine the floating potential of the plasma plume relative to the ground potential and to estimate electron density values. The emissive probe is used to define the plasma potential of the plasma plume relative to the ground potential. By combining data from both types of probes, the mean electron energy can be determined from the difference of plasma and floating potentials.

The voltage-current characteristics of the Langmuir and emissive probes are measured with a Keithley 2410 digital source measure unit. Heating the emissive probe is performed with a source measure unit Keithley 2450.

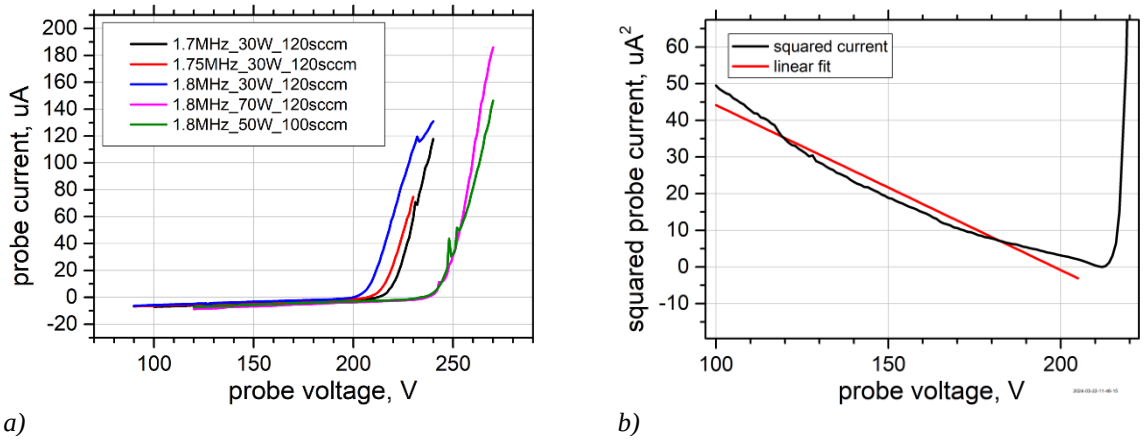

a) *b)*

Figure 4. Langmuir probe characteristics. Raw signal (a) and squared probe current example (b).

Both probes were tested at a distance of 2 cm from the C-STAR cutoff. The thruster was working on high mass flow operating points, to generate high density plume, easing the characterization of the same regime by the means of

optical diagnostic, due to its sensitivity. An example of the measurements done with the Langmuir probe are depicted on the figure 4(a).

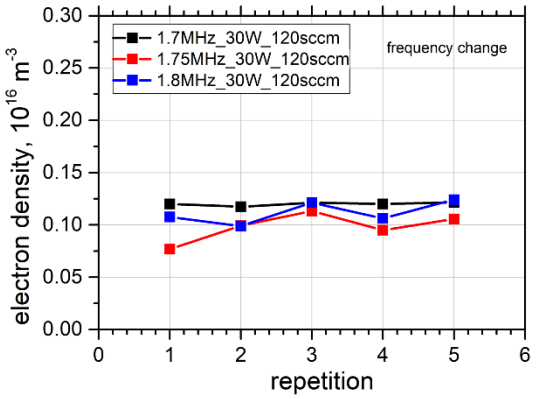

a)

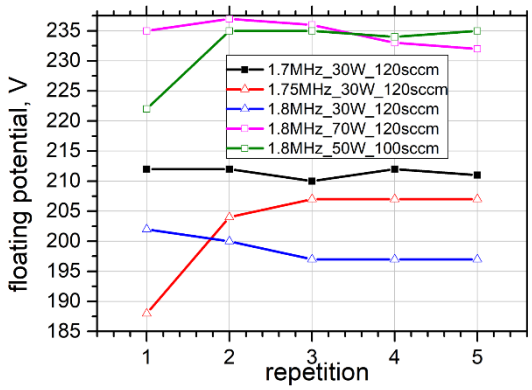

b)

Figure 5. Parameters of the C-Star plume at 2cm from the cutoff derived from the Langmuir probe measurements. Electron density (a) and floating potential (b).

Figure 4(b) shows that the squared probe current in the ionic part of the voltage-current characteristic exhibits a linear dependence on the probe voltage, validating the applicability of the Orbital Motion Limited (OML) theory[5].

The measurements resulted in electron number densities of approximately 10^{15} m^{-3} and a floating potential of 190-240 V. Each measurement was conducted multiple times to ensure reliability. The results are presented in Fig. 5.

The emissive probe was tested only under vacuum conditions, without plasma, showing a space potential of 0 V[6], as expected (see Fig. 6).

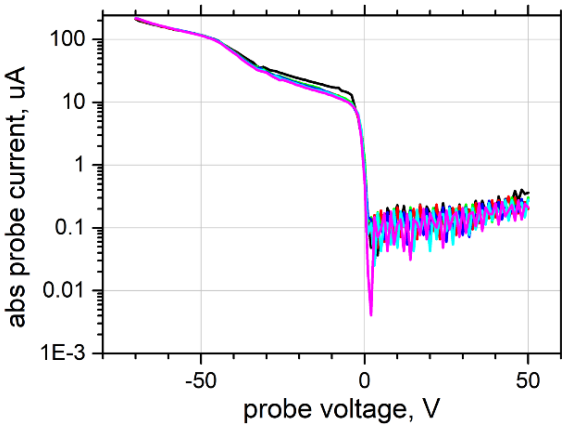

Figure 6. Results of measurements of emissive probes without plasma.

The complete determination of plasma parameters by probe diagnostics includes the determination of: a) plasma density from ion part of Langmuir VCC according to the procedures for the OML theory; b) the temperature of the electrons from the difference between the floating and plasma potentials; c) floating potential by the Langmuir and plasma potential by emissive probes.

B. Retarding potential analyser

A Retarding Potential Analyzer (RPA) is a plasma diagnostic tool that uses a series of electrostatic grids to selectively repel constituents of the plasma and a collector electrode to detect the ion energy distribution. The grids of the RPA are supplied with two stabilized power supplies (FUG MCP 35–1250 and FUG MCP 140–2000). The signal on the

a)

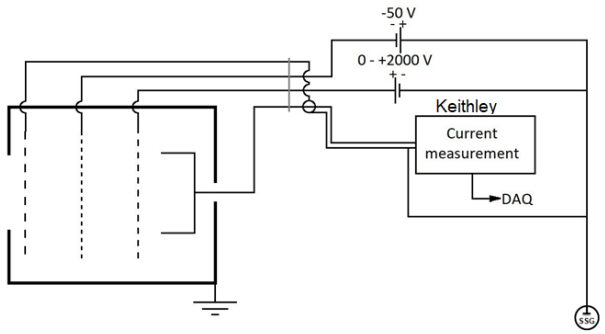

b)

Figure 7. Retarding potential analyser. General view (a) and electrical scheme (b).

collector is recorded with a Keithley 2410 source measure unit. The general view and the schematics are depicted on fig. 7.

Preliminary results of the ion energy distribution were gathered at three different power levels with a 120 sccm argon flow. The results clearly show average ion energies of 180, 330, and 410 eV corresponding to applied power levels of 53 W, 60 W, and 70 W, respectively (see fig.8).

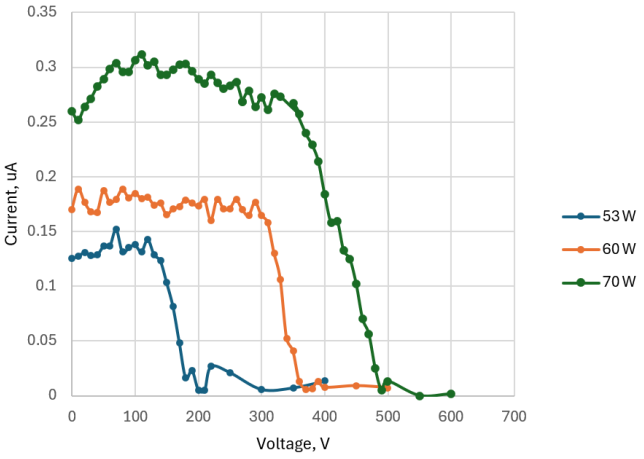

Figure 8. Raw signal of the RPA gathered from C-STAR at 120 sccm flow of argon.

IV. Optical diagnostic setup and preliminary results

The optical diagnostic setup and its preliminary results are described in this chapter. Rayleigh, and Thomson scattering techniques are employed for plasma characterization. Sensitivity issues are identified, mitigation approaches are proposed, and some are partially implemented.

A. Optical diagnostic setup

The laser scattering diagnostics uses an optical fibre-based setup to reduce stray laser radiation. The setup consists of two main parts: the laser delivery system and the optical detection system.

The laser delivery system involves coupling the beam to an optical fibre using a fibre port (PAF2s-18A, Thorlabs). A chopper is installed between the laser head and the fibre port. The optical fibre with an inner core of 100 µm is connected to the vacuum fibre feedthrough (VK4H2S, Thorlabs). The feedthrough has a core diameter of 200 µm, and the vacuum side is coupled to an optical fibre with a core diameter of 300 µm. All fibre connections are made using ADASMA (Thorlabs) mating sleeves, ensuring minimal laser power loss at coupling points. Measurements of the laser beam power at the vacuum side exit showed that this arrangement could deliver 85% of the energy.

In the detection system, the fibre inside the vacuum chamber is attached to the detector focusing unit, which includes a fibre holder and an achromatic lens (f=50 mm). Another part of the fibre guides the collected radiation through the vacuum feedthrough (VK4H4S, Thorlabs) to the atmospheric side fibre and the focusing unit in front of the spectrometer slit. Optionally, the fibre can be attached to a photomultiplier detector.

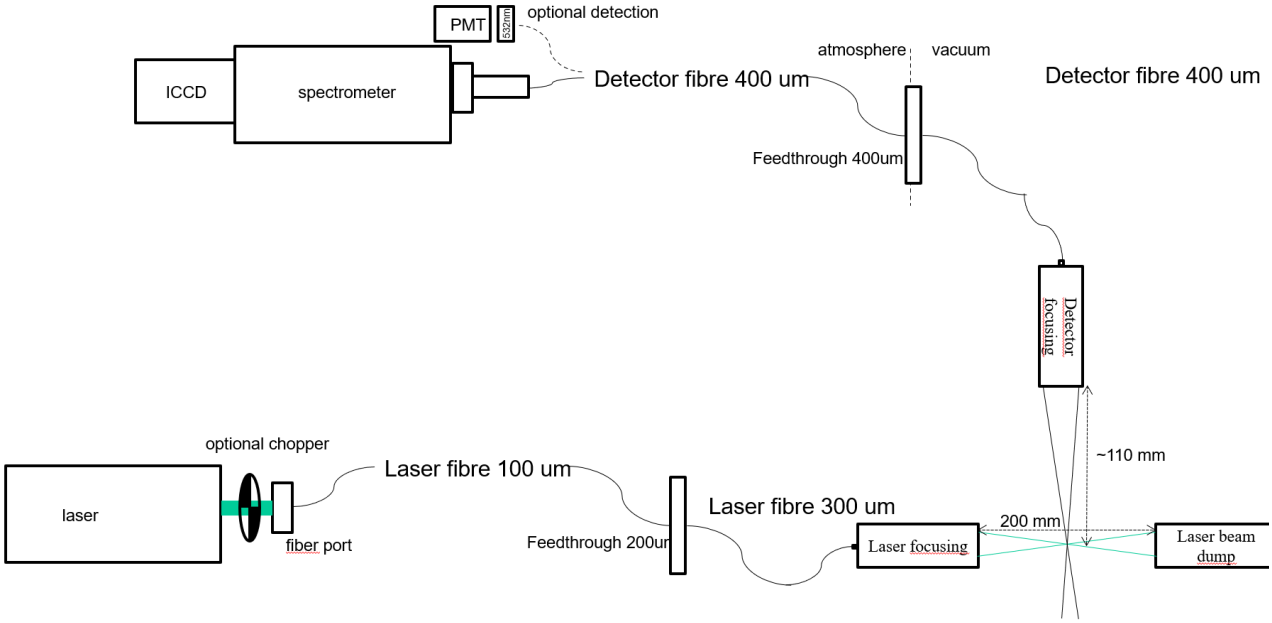

Figure 9. Scheme of optical diagnostic setup.

As mentioned in Chapter II-C, a rectangular frame is used to accommodate the diagnostic equipment inside the vacuum chamber. The laser fibre is attached to the laser focusing unit. To maintain a small focused spot size while

providing adequate distance between the unit and the thruster, a two-lens system is used. This system creates a focused beam with a diameter of approximately 2 mm at a distance of 20 cm from the last lens. Additional apertures are included to reduce stray light intensity from focusing surfaces. The final distance between the exit of the focusing unit and the focal point is about 12 cm.

Measurements of the laser power after installing the focusing optics showed that 75% of the incident laser radiation could be delivered to the focal spot. A beam trap is placed further along the laser beam path.

The laser focusing unit and the detector focusing unit are positioned at a 90-degree angle to each other. The system was calibrated using a reference radiation lamp with an integrating sphere (ISS-8P-HP-V01 from Gigahertz-Optik) and a stabilized current source (OL65A from Optronic Laboratories) to determine the absolute radiation.

B. Rayleigh scattering.

To ensure the reliability of the designed system, laser scattering measurements at atmospheric pressure were performed. The scattered signal was characterized as a function of laser power. Figure 10 shows the results of these measurements, with the power scanned from 10 mW to 2 W, demonstrating an almost linear dependence on the detected signal. Any deviation from this linear dependence would indicate problems with power transmission through the system.

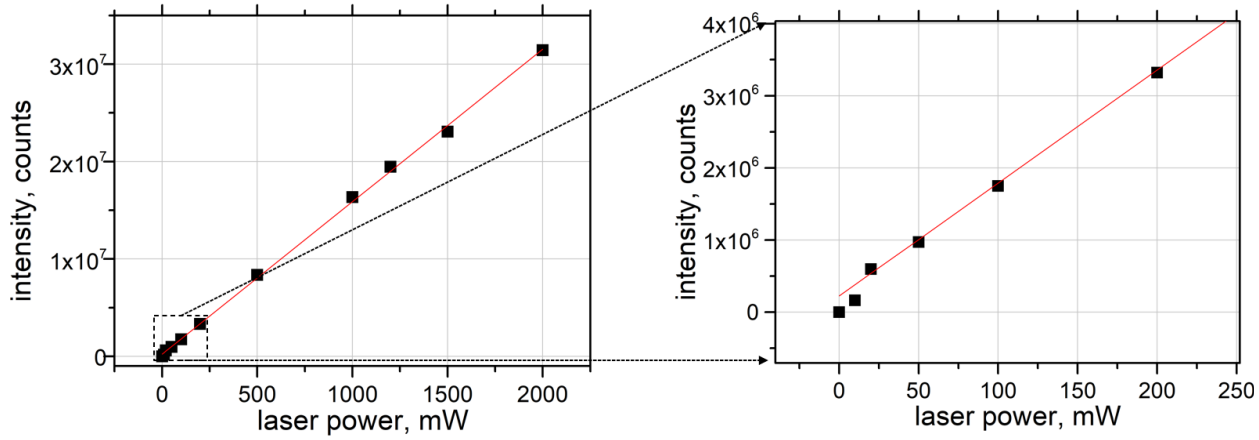

Figure 10. Laser power delivery test results.

Subsequently, a series of measurements were conducted to characterize the pressure in the chamber. The signal from the scattered laser was plotted against the pressure in the chamber (see Fig. 11). For convenience, the signal was normalized to the atmospheric pressure signal. Analysis of this data showed that pressures down to 10 mbar were easily detectable, but the signal at lower pressures plateaued. This sensitivity was below the requirements for the diagnostic setup, therefore activities to increase it were performed.

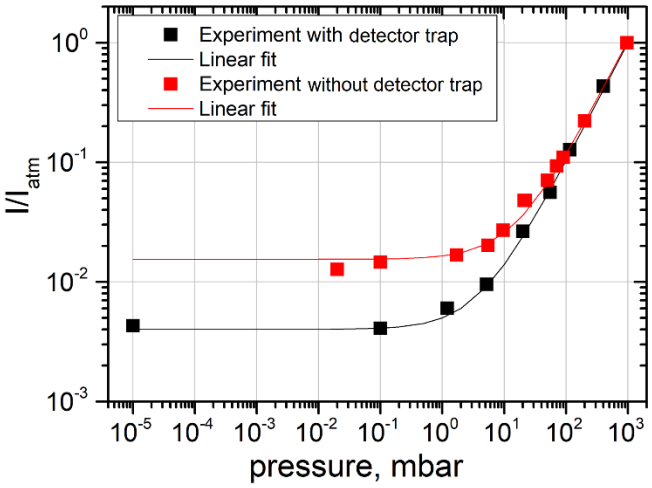

Figure 11. Reyleigh scattering signal measurements with and without detector trap.

One apparent reason for the low sensitivity of Rayleigh scattering could be the stray laser signal. Laser light not focused on the laser trap, or reflecting off it, was scattering from the metal walls of the chamber, creating background radiation and spoiling the results. To address this, an additional cylindrical trap (see trap ver.1 fig.12(b)) was installed opposite the detector focusing lenses. This modification improved the detectable threshold to 1 mbar.

While the implementation of the detector trap partially mitigated the stray laser effect on sensitivity, addressing the root cause was also necessary. The original laser trap (ver.0, see Fig. 12(a)) was a 25 mm diameter cylinder with a 15 mm aperture and a welding glass filter at the bottom. A substantial amount of laser light missed the trap, reflecting

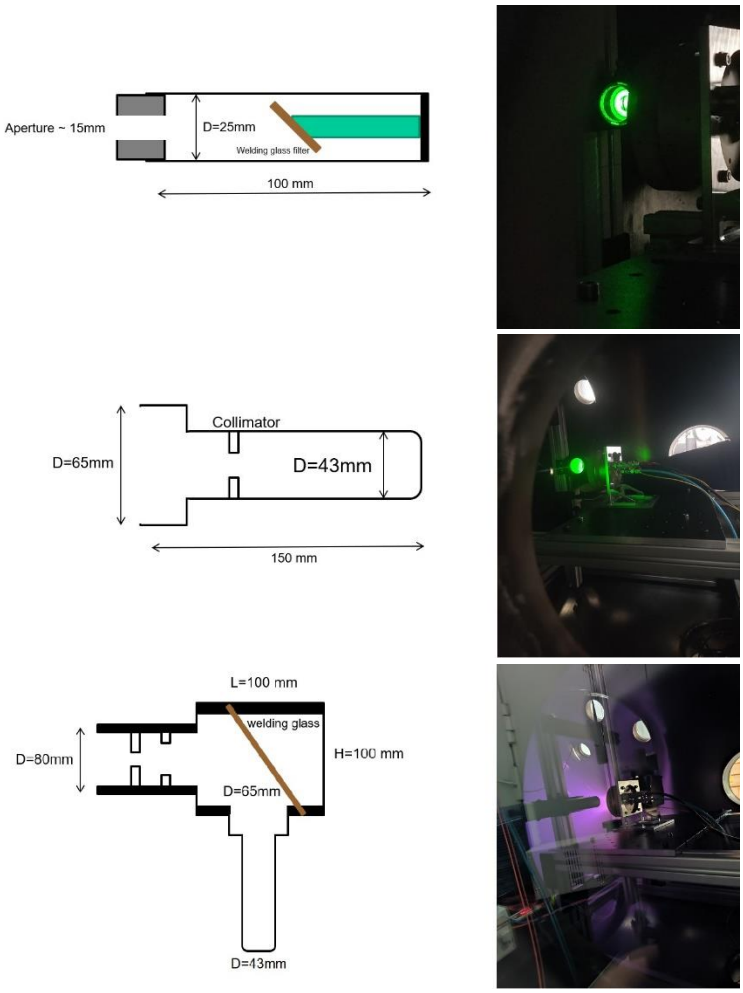

Figure 12. Laser traps constructions on the left and their pictures under test conditions on the right. Trap ver.0 with collimator and a filter-mirror (a), trap ver.1 with collimator and with coating (b) and trap ver.2 with collimator, coating and a filter.

off the chamber walls and re-entering the analysis zone. Additionally, the trap's absorptivity was not high enough, causing some laser light to reflect back into the analysis zone, thereby increasing noise and reducing measurement accuracy.

To address these issues, a larger and more efficient trap (ver.1) was manufactured. This new trap featured a 65 mm neck turning into a 43 mm inner diameter cylinder, fully coated with Musou Black Acrylic Paint with a light absorption coefficient of 99.4%. Inside the cylinder, a baffle with a 25 mm orifice was installed 20 mm from the entrance. This setup significantly reduced the amount of reflected laser light by ensuring that most stray light was absorbed within the trap.

Finally, a more advanced trap (ver.2) was developed, combining elements from both designs. This trap utilized an 80 mm inner diameter cylinder that captured the laser through two apertures with 15 mm and 25 mm diameter orifices. The laser beam was then reflected off a welding glass filter into the ver.1 trap, incorporated into the design at a 90-degree angle. This multi-stage trapping system further minimized the chances of laser light escaping back into the chamber, thus effectively reducing stray light and enhancing the system's overall sensitivity.

The effectiveness of these modifications is illustrated in Fig. 13.

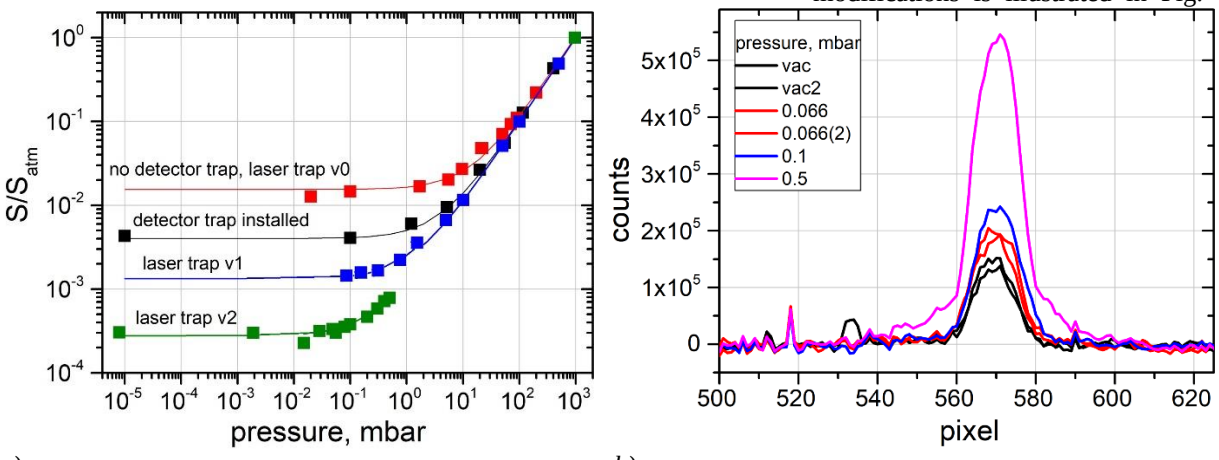

Figure 13. Reyleigh scattering signal measurements results with various trap configurations (a) and the raw data of the spectrometer (b).

The implementation of trap ver.1 improved sensitivity, allowing for the detection of pressures down to approximately 0.5 mbar. The advanced trap ver.2 further increased sensitivity, enabling the detection of pressures as low as 0.05 mbar. The raw data from the spectrometer of the final setup is depicted in Fig. 13(b), highlighting the improvement in measurement accuracy. Additionally, measurements of scattered signals from argon atoms at low pressures were conducted. Due to their similar cross-sections with air (5.46 × 10^-31 m^2 for argon vs 5.61 × 10^-31 m^2 for air), the signals nearly coincide, and thus, are not presented in this paper.

C. Thomson scattering

Thomson scattering is another measurement technique considered for this project. It operates by measuring the signal of laser light scattering on free electrons. The intensity of this scattered light is proportional to the electron density in the plasma, while its spectral width can be used to determine the electron temperature. Unlike Rayleigh scattering, the Thomson scattering signal is much broader and can typically be distinguished from the Rayleigh scattering signal.

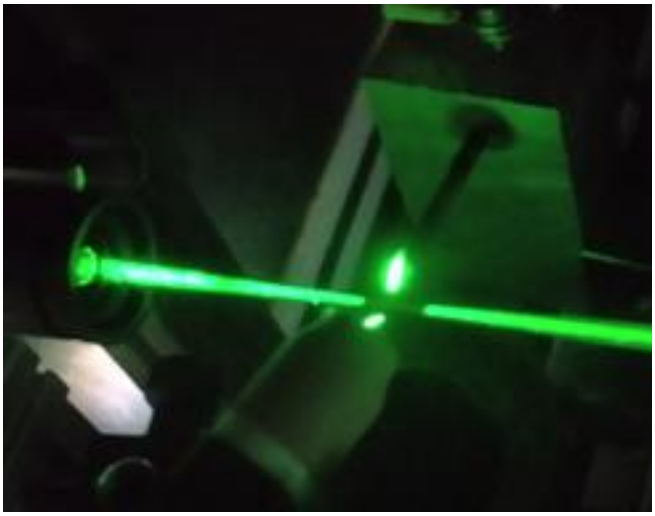

Figure 14. Test setup for electric arc measurements.

Several attempts to measure Thomson scattering in the plasma jet of the C-Star yielded no results. The signal was indiscernible against the strong background radiation. Various methods to reduce the background radiation were attempted without success. It was concluded that the sensitivity of the diagnostic setup was too low to detect the low-density plasma of the capacitive discharge. Consequently, the test object was switched to an electric arc discharge in argon (see Fig. 14). The current setup was unable to detect a signal from a 10 A arc, indicating that the diagnostic assembly was unsuitable for such

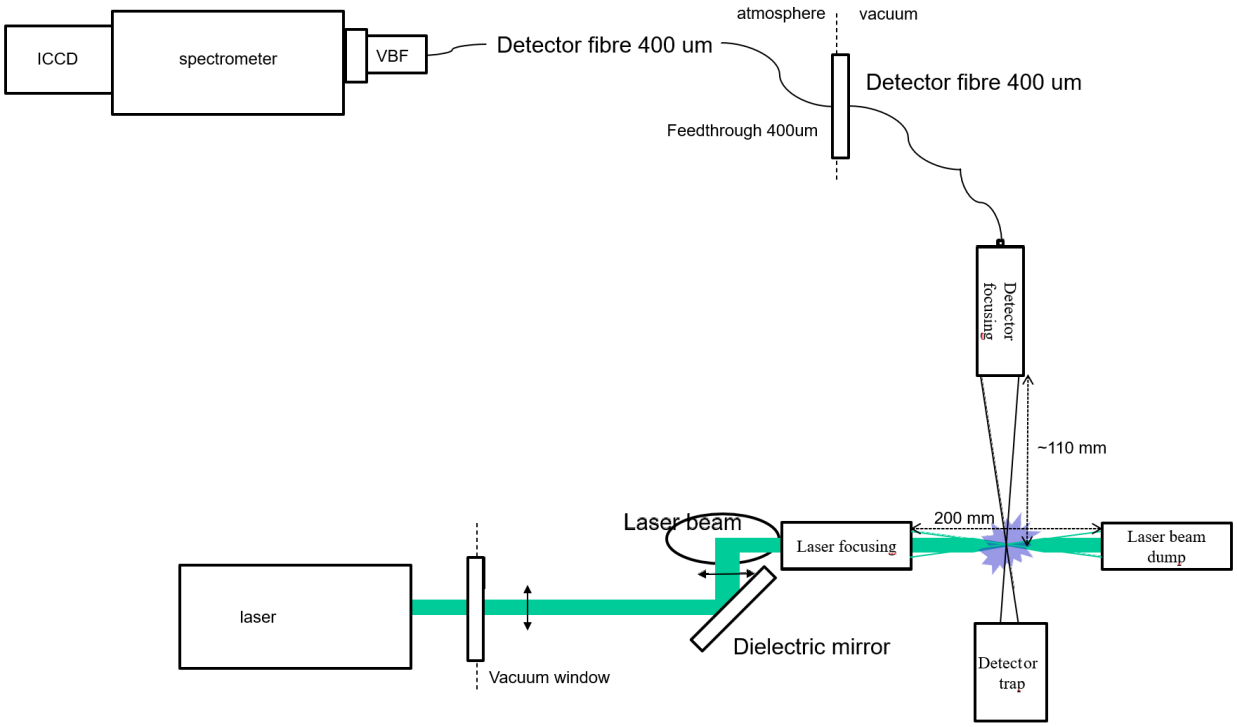

Figure 15. Scheme of modified optical diagnostic setup.

measurements. It was assumed that the optical radiation of the discharge itself interfered with the measurements. To address this problem, a modified setup was proposed (Fig. 15).

In the new setup, the continuous wave (CW) Verdi laser used previously was replaced with a pulsed Minilite laser, allowing measurements without the plasma radiation background due to shorter exposure times. The higher energy beam of the pulsed laser could not be delivered through the optical fiber and was instead directed using a set of dielectric mirrors and the window flange of the vacuum chamber. The setup makes use of the Volume Bragg gratings

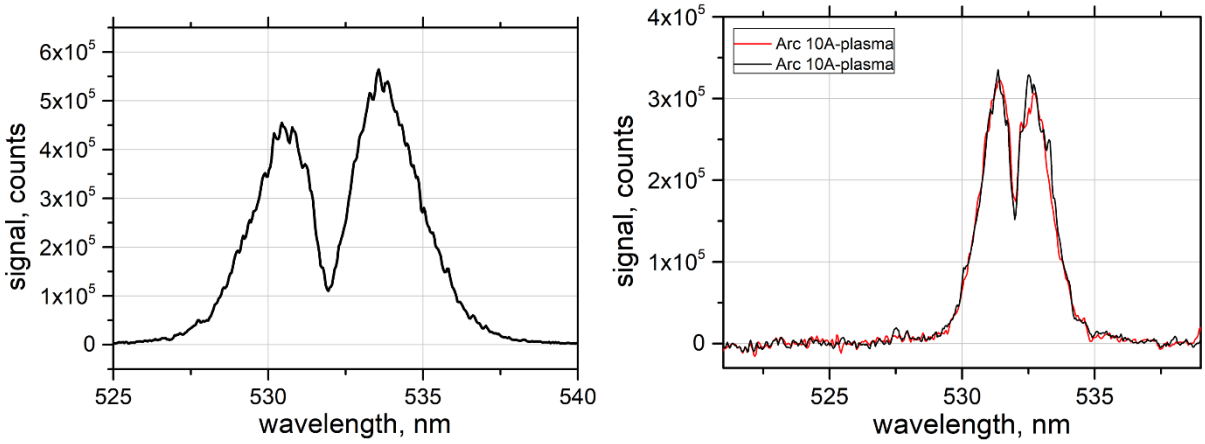

a) *b)*

Figure 16. Results of measurements with the modified optical setup. Raman scattering in air at atmospheric pressure (a) and the Thomson scattering in the 10 A arc in the argon (b)

filter to suppress the laser radiation at lasing wavelength and allow only the scattered radiation to be analysed. This eliminates the problems with background radiation introduced by stray laser reflections.

For absolute calibration, the Raman scattering signal in air was collected (Fig. 16(a)). With known values of air density (N_{air}) and scattering cross-section (σ_{dif}), it is possible to derive product of sensitivity (E), laser power (P) and observed laser beam length (L) from the equation:

$$I_{Raman}\left[\frac{counts}{nm}\right] = E\left[\frac{counts}{\frac{W}{sr}}\right] P[W]L[m]N_{air}[m^{-3}]\sigma_{dif}\left[\frac{m^2}{nmsr}\right] \quad (1)$$

The product EPL yields in $1{,}25*10^{14}$ [counts*m*sr] and is unique for our setup.

This product now can be used for determination of electron density from the similar equation for the Tomson scattering signal:

$$I_{Thomson}[counts] = E\left[\frac{counts}{\frac{W}{sr\ nm}}\right] P[W]L[m]N_e[m^{-3}]S_\lambda[nm^{-1}]\sigma_{Th}\left[\frac{m^2}{sr}\right] \quad (2)$$

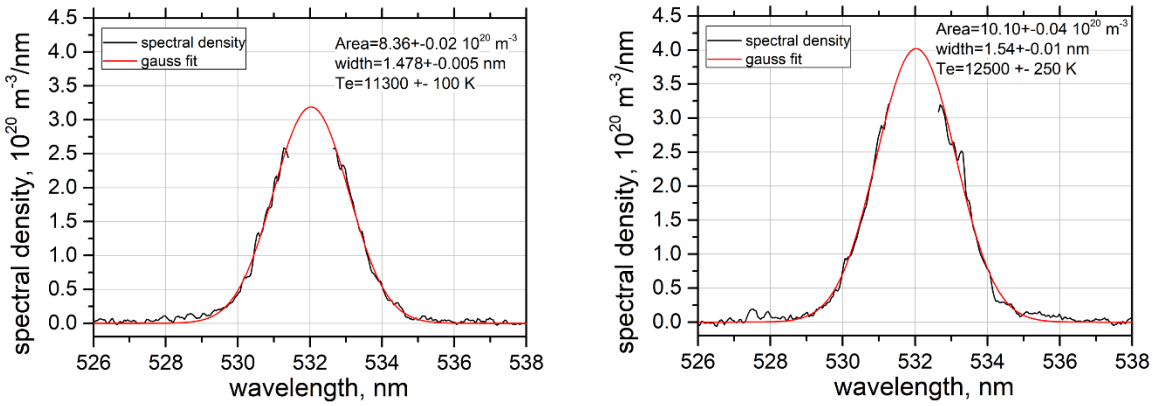

a) *b)*

Figure 17. Spectral density of electrons plots and estimated parameters for the 6 A (a) and 10 A (b) arcs in argon.

The electron density derived from this formula is:

$$N_e S_\lambda = \frac{I_{Thomson}}{EPL\sigma_{Th}} \tag{3}$$

The spectral distribution, plotted against the wavelength and approximated with a Gaussian fit, can then be used to determine the electron density as the area under the curve. Additionally, the electron temperature can be estimated from the spectral width[7]. Preliminary results for 10 A and 6 A arcs in argon are presented in figure 17.

V.Conclusion

A plasma diagnostic facility for EP systems was built and tested, incorporating various techniques such as Langmuir probes, emissive probes, retarding potential analysers, and Raman, Rayleigh, and Thomson scattering. These techniques are currently suitable for limited applications.

Due to the significant changes implemented in the setup during the preparation for Thomson scattering, it is necessary to reassess the feasibility of performing Rayleigh scattering with the newly introduced pulsed laser. One of the main requirements is the permanent assembly of the optical diagnostic setup. Furthermore, Thomson scattering should be performed on the original research object, the C-Star thruster. A rough sensitivity analysis, based on the measurements described in Chapter IV-C, indicates a detection limit of only 10^{18} m^{-3}, which is insufficient for characterizing capacitive discharge plasmas. Increasing the data accumulation time or switching to an even more powerful laser could improve this sensitivity. Additionally, the Intensified CCD (ICCD) used in the setup can implement water cooling to further reduce noise.

These and other enhancements to the test setup are already targeted for future research work and will be addressed in upcoming publications.

Acknowledgments

This work was supported by the ESA contract ESA/4000129121/19/NL/RA

References

[1]Vincent, B., Tsikata, S., Mazouffre, S., Minea, T., and Fils, J., "A Compact New Incoherent Thomson Scattering Diagnostic for Low-Temperature Plasma Studies," *Plasma Sources Science and Technology*, Vol. 27, No. 5, 2018, 055002. DOI: https://doi.org/10.1088/1361-6595/aabd13.

[2]Vincent, B., Tsikata, S., Mazouffre, S., and Boniface, C., "Thomson Scattering Investigations of a Low-Power Hall Thruster in Standard and Magnetically-Shielded Configurations," 36th International Electric Propulsion Conference, IEPC-2019-A-384, University of Vienna, Austria, Sept. 15-20, 2019.

[3] Smirnov, P., Kozakov, R., Schein, J. Experimental Characterization of the Capacitively Coupled RF-Plasma Thruster. Applied Sciences. Vol. 11, No. 15, p. 6799, 2021. DOI: 10.3390/app11156799.

[4]Smirnov, P. (2023). Development of the radiofrequency capacitively coupled plasma propulsion system. Poster presented at EPIC Electric Propulsion Workshop, Naples, Italy, May 9-12, 2023.

[5]Lobbia, R. B., & Beal, B. E. (2017). Recommended practice for use of Langmuir probe in electric propulsion testing. *Journal of Propulsion and Power*, 33, 566-581. doi:10.2514/1.B35531

[6]Sheenan, J. P., et al. (2017). Recommended Practice for use of Emissive Probes in Electric Propulsion Testing. *Journal of Propulsion and Power*, 33(3), 614. doi:10.2514/1.B35697

[7]Muraoka, K. (1998). Diagnostics of low-density glow discharge plasmas using Thomson scattering. *Plasma Physics and Controlled Fusion*, 40, 1221-1239.

[8]Godyak, V. A., & Alexandrovich, B. M. (2015). Comparative analyses of plasma probe diagnostics techniques. *Journal of Applied Physics*, 118, 233302. https://doi.org/10.1063/1.493689

[9]Miles, R. B., et al. (2001). Laser Rayleigh scattering. *Measurement Science and Technology*, 12, R33.

[10]Shardanand and Prasad Rao, A. D. (1977). Absolute Rayleigh scattering cross sections of gases and freons of stratospheric interest in the visible and ultraviolet regions. *NASA Technical Note* TN D-8422.